Drug-microenvironment mapping reveals resistance mechanisms and prognostic patient subgroups in CLL

Appendix

Peter-Martin Bruch*, Holly A. R. Giles*, Carolin Kolb , Sophie A. Herbst, Tina Becirovic, Tobias Roider, Junyan Lu, Sebastian Scheinost, Lena Wagner, Jennifer Huellein, Ivan Berest, Mark Kriegsmann, Katharina Kriegsmann, Christiane Zgorzelski, Peter Dreger, Judith B. Zaugg, Carsten Müller-Tidow, Thorsten Zenz, Wolfgang Huber*, Sascha Dietrich* * These authors contributed equally to this work.

4th April 2022

Contents

Appendix Methods

ATAC sequencing

Peripheral blood was taken from 4 CLL patients and separated by Ficoll gradient (GE Healthcare), mononuclear cells were cryopreserved on liquid nitrogen. Samples were later thawed from frozen as previously described[1] and MACS sorted for CD19 positive cells (Miltenyi autoMACS®). The cells were resuspended in RPMI (GIBCO, Cat.No. 21875–034), with the addition of 2mM glutamine (GIBCO, Cat.No. 25030–24), 1% Pen/Strep (GIBCO, Cat.No. 15140–122) and 10% pooled, heat–inactivated and sterile filtered human type AB male off the clot serum (PAN Biotech, Cat.No. P40–2701, Lot.No:P–020317). 5ml of cell suspension was cultured in 6–well plates (Greiner Bio–One Cat.No. 657160). After thawing, cells were incubated at 37°C and 5% CO2 for 6 hours in 0.2% DMSO. The final cell concentration was 2x10ˆ6 cells/ml. Cell viability and purity was assessed using FACS. All samples had a viability over 90% and over 95% of CD19+/CD5+/CD3– cells.

ATAC sequencing library generation

ATACseq libraries were generated as described previously[2]. Cell preparation and transposition was performed according to the protocol, starting with 5x10ˆ4 cells per sample. Purified DNA was stored at −20°C until library preparation was performed. To generate multiplexed libraries, the transposed DNA was initially amplified for 5x PCR cycles using 2.5 µL each of 25 µM PCR Primer 1 and 2.5 µL of 25 µM Barcoded PCR Primer 2 (included in the Nextera index kit, Illumina, San Diego, CA, USA), 25 µL of NEBNext High-Fidelity 2x PCR Master Mix (New England Biolabs, Boston, Massachusetts) in a total volume of 50 µL. 5 µL of the amplified DNA was used to determine the appropriate number of additional PCR cycles using qPCR. Additional number of cycles was calculated through the plotting of the linear Rn versus cycle, and corresponds to one-third of the maximum fluorescent intensity. Finally, amplification was performed on the remaining 45 µL of the PCR reaction using the optimal number of cycles determined for each library by qPCR (max. 13 cycles in total). The amplified fragments were purified with two rounds of SPRI bead clean-up (1.4x). The size distribution of the libraries was assessed on Bioanalyzer with a DNA High Sensitivity kit (Agilent Technologies, Santa Clara, CA), concentration was measured with Qubit® DNA High Sensitivity kit in Qubit® 2.0 Flurometer (Life Technologies, Carlsbad, CA). Sequencing was performed on NextSeq 500 (Illumina, San Diego, CA, USA) using 75bp paired-end sequencing, generating approx. 450 million paired-reads per run, with an average of 55 million reads per sample.

ATAC sequencing analysis of transcription factor activity in trisomy 12 CLL

Raw ATACseq data generated from our CLL samples were processed as described in Berest et al. 2019[3], with the only exception that we did not use CG bias correction step. We then used analytical mode of diffTF with HOCOMOCO v10 database[4] using the following parameters: minOverlap = 1; design formula = "~ Patient + trisomy 12 status".

Drug-stimulation profiling of samples treated with Ibrutinib, IL4 and AS1517499

The experiment in Appendix Fig. 20, was performed as detailed in the main methods (Sample preparation and drug-stimulation profiling), but with the following adjustments. 16 independent CLL PBMC samples were used and luminescence was read out using a Perkin Elmer EnSight.

Appendix Tables

Patient ID	Sex	Treated before	IGHV status	Methylation Cluster	Del13q	Del11q	Trisomy 12	Del17p
Pat_001	f	1	U	LP	1	0	0	0
Pat_002	m	1	M	IP	1	0	0	0
Pat_003	m	0	M	HP	0	0	1	0
Pat_004	f	1	U	LP	0	1	0	0
Pat_005	m	0	U	LP	1	0	0	0
Pat_006	f	0	U	LP	0	0	0	0
Pat_007	f	0	M	HP	1	0	0	0
Pat_008	m	1	U	LP	1	0	0	0
Pat_009	m	1	U	LP	1	0	0	1
Pat_010	f	1	U	LP	1	0	0	1
Pat_011	f	0	U	NA	0	0	1	0
Pat_012	f	0	M	HP	1	0	0	0
Pat_013	f	1	U	IP	1	1	0	0
Pat_014	m	0	M	HP	0	0	0	0
Pat_015	m	0	M	HP	1	0	0	0
Pat_016	m	0	M	HP	1	0	0	0
Pat_017	m	0	M	NA	1	0	0	0
Pat_018	f	1	U	LP	1	1	0	0
Pat_019	m	0	M	HP	1	0	0	0
Pat_020	f	1	M	IP	1	0	0	0
Pat_021	m	0	U	LP	0	0	0	1
Pat_022	f	0	M	IP	0	0	1	0
Pat_023	f	0	M	HP	0	0	0	0
Pat_024	f	1	M	HP	0	0	0	1
Pat_025	m	0	M	IP	1	0	0	0
Pat_026	m	0	M	HP	1	0	0	0
Pat_027	f	0	M	HP	1	0	0	0
Pat_028	f	0	M	IP	1	0	0	0
Pat_029	f	0	M	HP	1	0	0	0
Pat_030	m	1	M	HP	1	0	0	0
Pat_031	m	0	M	HP	0	0	0	0
Pat_032	f	1	U	LP	1	1	0	0
Pat_033	m	1	U	IP	0	1	0	0
Pat_034	m	1	U	LP	0	1	0	0
Pat_035	m	0	M	HP	1	0	0	0
Pat_036	m	1	U	LP	1	1	0	1
Pat_037	f	1	U	IP	1	0	0	0
Pat_038	m	0	M	IP	1	0	0	0
Pat_039	m	1	M	HP	1	0	0	0
Pat_040	f	0	M	HP	0	0	0	0
Pat_041	f	1	U	LP	0	0	1	0
Pat_042	f	0	M	IP	1	1	0	0
Pat_043	f	0	M	HP	1	0	0	0
Pat_044	m	0	M	HP	1	0	0	0
Pat_045	m	0	U	LP	0	0	0	0
Pat_046	m	0	M	IP	0	0	1	0
Pat_047	m	0	M	HP	1	0	0	0
Pat_048	m	0	M	HP	1	0	0	0
Pat_049	f	0	M	IP	0	1	0	0
Pat_050	m	0	M	HP	0	0	1	0
Pat_051	m	0	M	NA	1	0	0	0
Pat_052	f	0	M	IP	1	0	0	0
Pat_053	m	1	U	LP	1	1	0	0
Pat_054	f	1	U	LP	0	1	0	0
Pat_055	m	1	U	LP	0	0	0	0
Pat_056	f	0	U	LP	NA	NA	NA	NA
Pat_057	f	0	M	HP	1	0	1	0
Pat_058	f	1	U	LP	0	0	0	0

(continued)

Patient ID	Sex	Treated before	IGHV status	Methylation Cluster	Del13q	Del11q	Trisomy 12	Del17p
Pat_059	m	0	M	HP	1	0	0	0
Pat_060	m	1	M	IP	1	0	0	1
Pat_061	m	0	U	LP	0	0	1	0
Pat_062	m	1	U	LP	1	1	0	0
Pat_063	f	0	U	LP	1	0	0	0
Pat_064	m	1	U	LP	1	1	0	1
Pat_065	m	0	U	LP	0	1	0	0
Pat_066	m	1	U	LP	1	1	0	0
Pat_067	f	0	M	HP	1	0	0	0
Pat_068	m	0	M	HP	1	0	0	0
Pat_069	m	1	M	HP	1	0	0	0
Pat_070	f	0	M	HP	0	0	0	0
Pat_071	f	0	U	LP	0	0	0	0
Pat_072	m	1	M	HP	0	0	1	0
Pat_073	f	0	U	LP	1	1	0	0
Pat_074	f	0	M	HP	0	0	0	0
Pat_075	f	0	M	HP	1	0	0	0
Pat_076	m	0	M	HP	1	0	0	0
Pat_077	f	0	U	NA	0	0	1	0
Pat_078	m	0	U	LP	0	0	0	0
Pat_079	m	0	M	HP	1	0	0	0
Pat_080	f	0	M	HP	0	0	0	0
Pat_081	m	0	M	HP	0	0	0	0
Pat_082	m	0	U	LP	0	0	0	0
Pat_083	m	0	M	HP	0	0	0	0
Pat_084	m	0	U	LP	0	0	1	0
Pat_085	m	0	M	HP	0	0	0	0
Pat_086	m	1	U	LP	1	1	0	0
Pat_087	m	0	M	IP	1	0	0	0
Pat_088	f	1	U	LP	1	0	0	1
Pat_089	m	0	M	HP	0	0	0	0
Pat_090	m	1	U	LP	0	0	1	0
Pat_091	m	1	M	NA	1	0	0	0
Pat_092	m	1	M	HP	0	0	0	0
Pat_093	m	0	M	HP	1	0	0	0
Pat_094	f	1	M	HP	0	0	0	0
Pat_095	m	1	U	LP	0	0	0	0
Pat_096	m	0	M	HP	0	0	0	0
Pat_097	f	1	U	LP	0	0	0	0
Pat_098	m	0	M	HP	1	0	0	0
Pat_099	f	0	U	LP	1	0	0	0
Pat_100	f	0	U	LP	1	0	0	0
Pat_101	f	0	U	LP	1	0	0	0
Pat_102	m	1	U	IP	0	0	0	0
Pat_103	f	0	M	HP	1	0	1	0
Pat_104	f	1	M	HP	0	0	0	0
Pat_105	m	0	U	LP	NA	NA	NA	NA
Pat_106	m	0	U	LP	1	1	0	1
Pat_107	f	0	M	NA	1	0	0	0
Pat_108	m	0	M	NA	1	0	1	0
Pat_109	m	0	M	HP	1	0	0	0
Pat_110	m	0	M	IP	1	1	0	0
Pat_111	f	1	U	LP	1	0	0	0
Pat_112	f	0	M	NA	0	0	1	0
Pat_113	f	0	M	HP	1	0	0	0
Pat_114	m	0	U	LP	1	0	0	0
Pat_115	m	1	U	LP	1	0	0	1
Pat_116	m	0	U	LP	1	0	0	0
Pat_117	m	0	U	IP	1	0	0	0
Pat_118	f	0	M	HP	0	0	0	1

(continued)

Patient ID	Sex	Treated before	IGHV status	Methylation Cluster	Del13q	Del11q	Trisomy 12	Del17p
Pat_119	m	0	U	LP	NA	NA	NA	NA
Pat_120	f	0	U	LP	0	0	1	0
Pat_121	m	0	U	LP	0	0	0	1
Pat_122	m	0	U	LP	0	1	0	0
Pat_123	m	0	U	LP	1	0	0	1
Pat_124	f	0	M	HP	1	0	1	0
Pat_125	f	0	M	HP	1	0	0	0
Pat_126	m	1	NA	NA	0	0	1	0
Pat_127	m	0	U	LP	1	1	0	1
Pat_128	m	0	M	HP	1	0	0	0
Pat_129	m	1	U	LP	1	0	0	0
Pat_130	f	0	M	IP	1	0	0	0
Pat_131	f	0	U	LP	1	0	0	1
Pat_132	m	1	U	LP	1	0	0	1
Pat_133	m	1	U	LP	1	0	0	1
Pat_134	m	1	M	HP	1	0	0	1
Pat_135	m	0	M	HP	1	0	0	0
Pat_136	m	0	M	HP	1	0	0	0
Pat_137	f	0	U	LP	0	0	1	0
Pat_138	f	0	M	HP	1	0	0	0
Pat_139	f	0	M	HP	NA	NA	NA	NA
Pat_140	f	0	M	IP	1	0	0	0
Pat_141	m	0	M	IP	1	0	0	0
Pat_142	m	0	M	HP	1	0	0	0
Pat_143	f	0	U	LP	1	0	0	0
Pat_144	m	1	U	LP	0	0	0	1
Pat_145	f	0	M	HP	0	0	0	0
Pat_146	m	1	U	LP	NA	NA	NA	NA
Pat_147	m	1	U	LP	0	0	0	1
Pat_148	m	1	U	NA	1	0	0	0
Pat_149	m	1	U	LP	0	1	1	0
Pat_150	f	0	M	HP	1	0	0	NA
Pat_151	m	0	U	LP	0	0	1	0
Pat_152	m	0	NA	NA	0	1	1	0
Pat_153	m	1	U	LP	1	0	0	0
Pat_154	m	0	M	HP	1	0	0	0
Pat_155	m	0	M	HP	1	0	0	0
Pat_156	f	0	U	LP	1	0	0	0
Pat_157	f	0	U	LP	1	1	0	0
Pat_158	m	0	M	HP	1	0	0	0
Pat_159	f	0	U	LP	1	0	0	0
Pat_160	m	0	U	LP	NA	NA	NA	NA
Pat_161	m	1	U	LP	0	0	0	0
Pat_162	m	0	M	HP	0	0	0	0
Pat_163	m	0	M	HP	0	0	0	0
Pat_164	f	0	U	LP	0	0	0	0
Pat_165	m	1	U	LP	0	1	1	0
Pat_166	m	0	U	LP	1	0	1	0
Pat_167	m	0	NA	IP	NA	NA	NA	NA
Pat_168	m	0	M	HP	1	1	0	0
Pat_169	m	0	M	HP	0	0	1	0
Pat_170	m	0	M	HP	1	0	0	0
Pat_171	m	0	M	HP	1	0	0	0
Pat_172	m	0	M	HP	1	0	0	0
Pat_173	m	0	M	HP	1	0	0	0
Pat_174	f	0	U	LP	NA	0	NA	0
Pat_175	m	0	U	LP	0	0	0	0
Pat_176	f	0	M	HP	NA	NA	NA	NA
Pat_177	f	0	NA	IP	NA	1	NA	NA
Pat_178	m	0	M	HP	1	0	0	0

(continued)

Patient ID	Sex	Treated before	IGHV status	Methylation Cluster	Del13q	Del11q	Trisomy 12	Del17p
Pat_179	m	0	U	LP	0	1	0	0
Pat_180	m	0	M	HP	NA	NA	NA	NA
Pat_181	f	0	M	HP	NA	NA	NA	NA
Pat_182	m	0	M	HP	1	0	0	0
Pat_183	f	1	NA	IP	1	0	0	0
Pat_184	m	0	U	LP	NA	NA	NA	NA
Pat_185	m	0	M	HP	NA	NA	NA	NA
Pat_186	m	0	M	HP	1	0	0	0
Pat_187	m	1	U	LP	NA	NA	NA	NA
Pat_188	m	0	NA	NA	NA	NA	NA	NA
Pat_189	m	0	NA	NA	NA	NA	NA	NA
Pat_190	m	0	NA	NA	NA	NA	NA	NA
Pat_191	f	0	NA	NA	0	0	0	0
Pat_192	f	0	NA	NA	1	0	0	0

Appendix Table 1. Patient samples included in the study.

List of patient samples and selected characteristics. For a full list of characteristics see online vignette.

Genetic_alteration	Wildtype/IGHV unmutated	Mutated/ IGHV Mutated	Not available
ATM	164	16	12
BIRC3	177	3	12
CARD11	135	3	54
CREBBP	135	3	54
CSMD3	175	5	12
del11p	143	3	46
del11q	148	28	16
del12q	171	3	18
del13q	66	108	18
del14q	145	5	42
del15q	141	5	46
del17p	154	20	18
del17q	143	3	46
del18p	141	5	46
del1q	141	5	46
del21q	143	3	46
del3p	143	3	46
del3q	143	3	46
del4p	143	3	46
del4q	143	3	46
del6q	166	7	19
del7q	143	3	46
del8p	135	11	46
del9p	140	6	46
del9q	142	4	46
EGR2	176	4	12
FAT2	175	5	12
FAT4	176	4	12
FBXW7	178	3	11
FLRT2	135	3	54
gain17q	143	3	46
gain18q	144	4	44
gain19p	142	4	46
gain19q	142	4	46
gain1q	143	3	46
gain2p	137	9	46
gain8q	159	13	20
IGHV.status	83	99	10
IKZF3	176	4	12
MED12	170	10	12
MYD88	184	3	5
NFKBIE	175	5	12
NOTCH1	137	24	31
POT1	174	6	12
Ras_Raf	170	15	7
RYR2	177	3	12
SF3B1	161	26	5
SPEN	177	3	12
TP53	157	30	5
trisomy12	149	25	18
U1	137	5	50
XPO1	175	5	12
ZMYM3	134	4	54

Appendix Table 2. List of genetic alterations tested for their association with stimuli response in the univariate model of Figure 3A.

Only genetic alterations with at least 3 positive cases were considered.

Factor	HR	p value	CI Low	CI High
Cluster 3 vs Cluster 1	0.95	0.87	0.53	1.72
Cluster 3 vs Cluster 2	1.56	0.26	0.72	3.41
Cluster 3 vs Cluster 4	0.35	0.02	0.14	0.87
IGHV.status	2.04	0.28	0.55	7.50
trisomy 12	0.99	0.98	0.48	2.07
TP53	4.12	<0.0001	2.42	7.02
Methylation_ClusterIP	1.47	0.37	0.63	3.42
Methylation_ClusterLP	0.93	0.92	0.23	3.74

Appendix Table 3. Multivariate survival analysis of response clusters.

Multivariate Cox proportional hazards model of stimuli response clusters and genetic subgroups of disease progression using TTT and C3 as reference.

Factor	HR	p value	CI Low	CI High
Cluster 3 vs Cluster 1	1.27	0.37	0.75	2.16
Cluster 3 vs Cluster 2	2.06	0.03	1.07	3.93
Cluster 3 vs Cluster 4	0.35	0.01	0.17	0.73

Appendix Table 4. Survival analysis of microenvironmental response clusters comparing Cluster 3 to the other Clusters.

Factor	HR	p value	CI Low	CI High
Cluster 3 vs combined Clusters 1 and 2 , ”3”	1.42	0.17	0.86	2.36

Appendix Table 5. Survival analysis of microenvironmental response clusters comparing Cluster 3 to the combined Cluster 1 and 2.

	Pathway	Geneset Database	Geneset Size	Spi-B targets (/333)	SPIB p-value	SPIB adj. p-value
JAK STAT signaling pathway	JAK STAT signaling pathway	KEGG	155	8	0.005	0.099

Appendix Table 6. Over-representation test of immune signalling pathways (and control pathways) amongst Spi-B gene targets, based on primary CLL ATACseq data.

Spi-B gene targets defined as nearest gene to each Spi-B binding site. Spi-B binding sites subset from all Spi-B sites defined in the HOCOMOCO database, and subset for those that that show an absolute Log2 fold change > 1 and a p value < 0.1 in trisomy 12 versus non-trisomy 12 CLL. Log2FC values and p values calculated using the diffTF package based on the CLL ATACseq data from Rendeiro et al. 2016.

	Pathway	Geneset Database	Geneset Size	Spi-B targets (/10974)	SPIB adj. p-value	SPIB adj. p-value
Signaling by Interleukins	Signaling by Interleukins	Reactome	463	293	0.000	0.001
BCR Signaling Pathway	BCR Signaling Pathway	KEGG	75	56	0.000	0.004
TLR Signaling Pathway	TLR Signaling Pathway	KEGG	102	73	0.000	0.004
TCR Signaling Pathway	TCR Signaling Pathway	KEGG	108	74	0.003	0.018
Interleukin 4 and Interleukin 13 Signaling	Interleukin 4 and Interleukin 13 Signaling	Reactome	111	74	0.009	0.043
Chemokine Signaling Pathway	Chemokine Signaling Pathway	KEGG	189	120	0.011	0.046
Interleukin 6 Signaling	Interleukin 6 Signaling	Reactome	11	10	0.015	0.050
Signaling by TGFbeta Receptor Complex	Signaling by TGFbeta Receptor Complex	Reactome	75	51	0.016	0.050
Interleukin 15 Signaling	Interleukin 15 Signaling	Reactome	14	12	0.018	0.050
JAK STAT signaling pathway	JAK STAT signaling pathway	KEGG	155	98	0.024	0.061
Interleukin 10 Signaling	Interleukin 10 Signaling	Reactome	46	32	0.034	0.077

Appendix Table 7. Over-representation test of immune signalling pathways (and control pathways) amongst Spi-B gene targets, based on DLBCL ChIPseq data.

Spi-B gene targets defined as nearest gene to each Spi-B binding site. Spi-B binding sites determined using ChIPseq data from Care et al 2014.

Appendix Figures

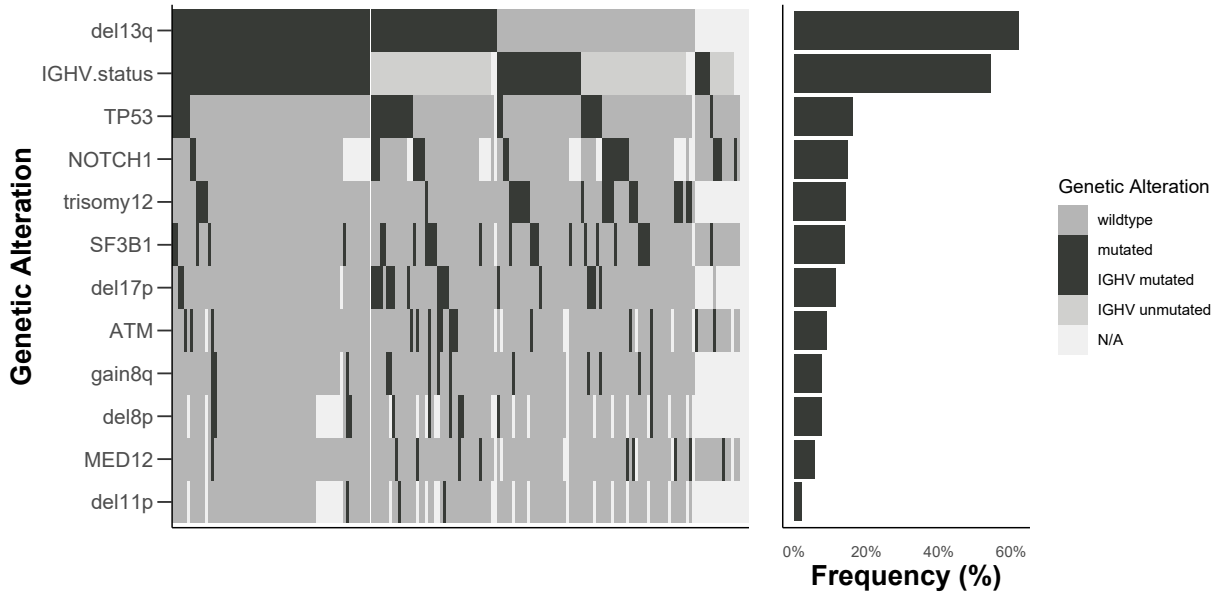

Appendix Figure 1. Genetic profiles of screened patient samples.

Selected genetic alterations on y-axis and screened patient samples on x-axis.

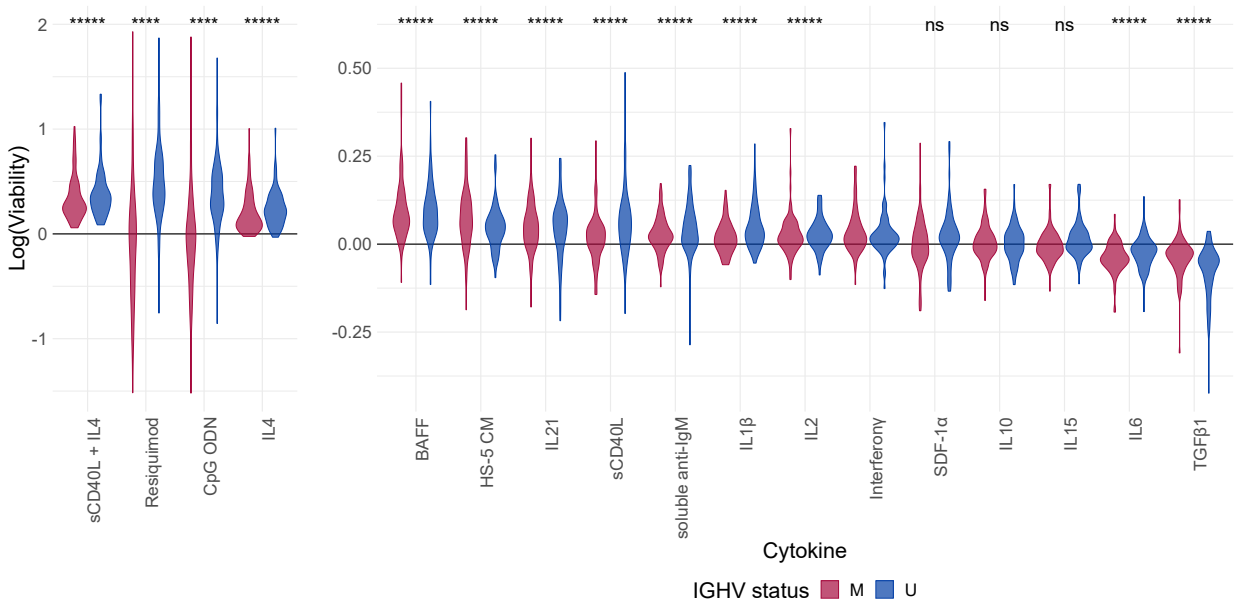

Appendix Figure 2. Response to stimuli by IGHV status.

Viability after 48h incubation with microenvironmental stimuli. Log transformed viabilities, normalized to DMSO solvent controls, stratified by IGHV status. BH-adjusted p-values are shown from one-sample t-tests of all patient samples. (p<0.00001=*****, p<0.0001=****, p>0.05=ns)

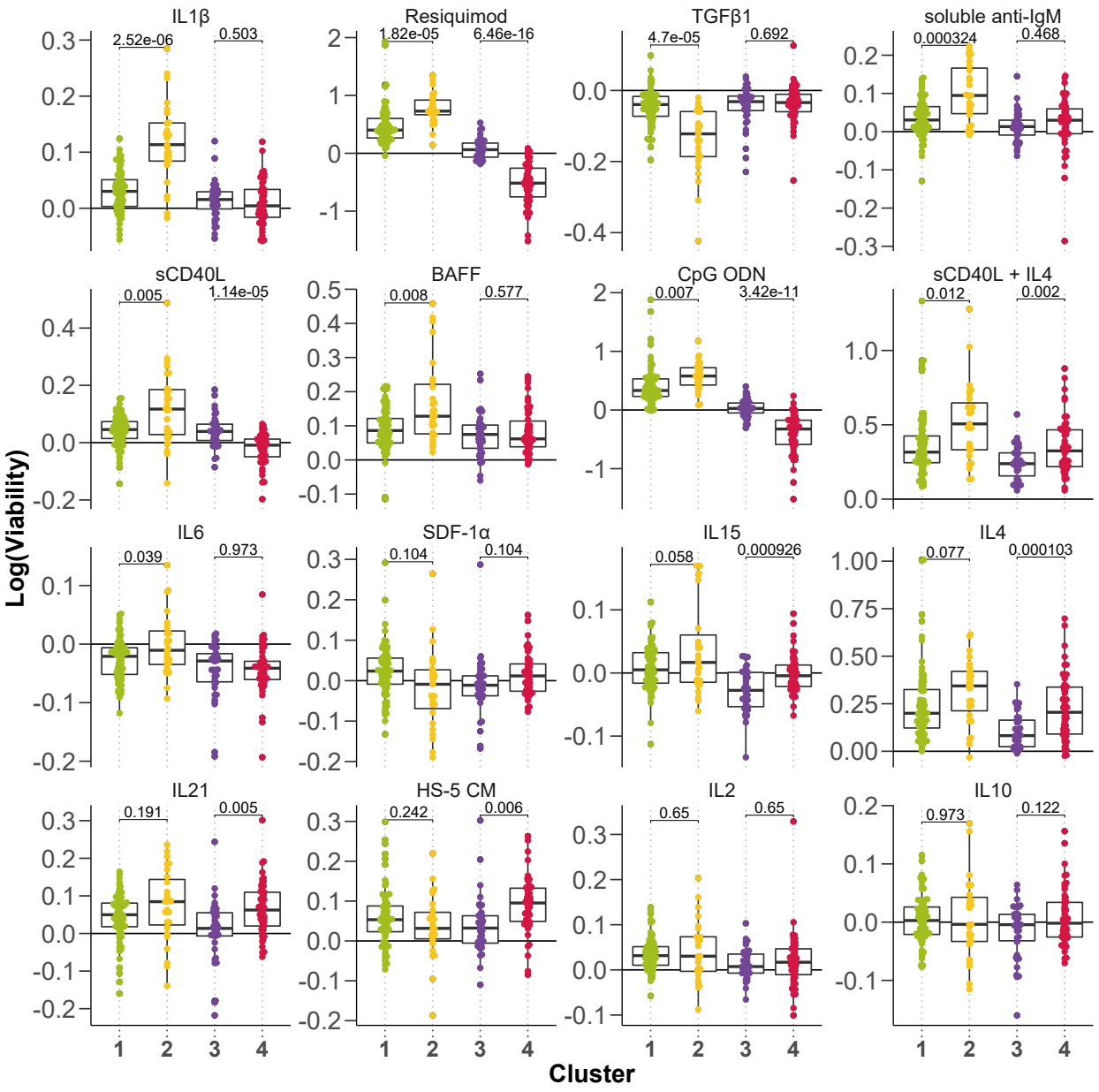

Appendix Figure 3. Stimuli response by clusters.

Log transformed viabilities after treatment with stimuli, faceted by cluster. BH-adjusted p-values from student's t-tests are shown.

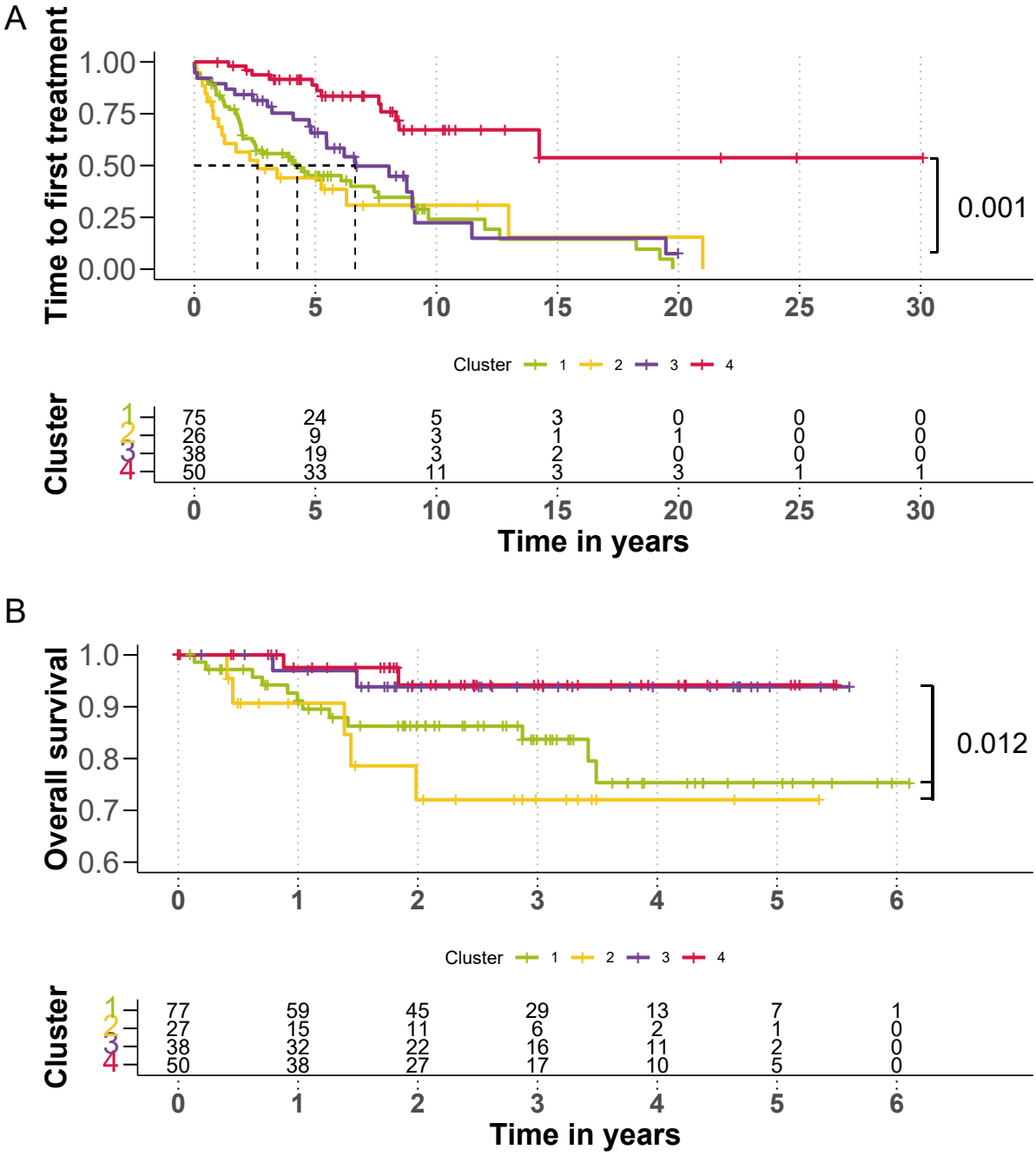

Appendix Figure 4. Time to first treatment and overall survival by clusters.

Kaplan-Meier Curves of time to first treatment with p-value from univariate Cox proportional hazards model between C3 and C4 **(A)** and overall survival with p-value from univariate Cox proportional hazards model between C1&2 and C3&4 **(B)**. Median survival not reached.

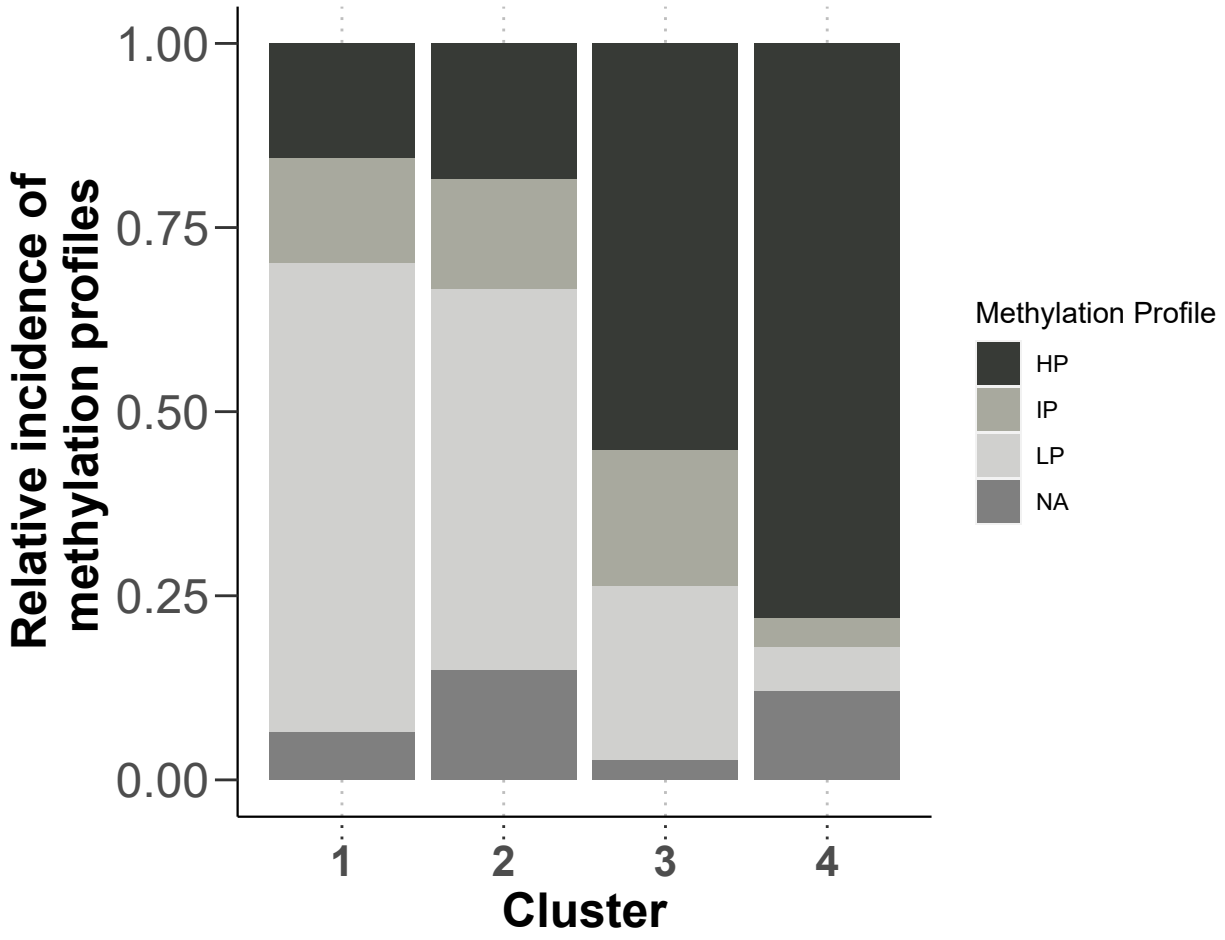

Appendix Figure 5. Methylation profile of Clusters defined by response to microenvironmental stimuli

Barplot of methylation profiles in the four clusters of microenvironmental response. Predominantly IGHV unmutated clusters 1 and 2 show higher abundance of Low programmed Methylation profiles, while predominantly IGHV mutated clusters 3 and 4 show more highly programmed methylation clusters.

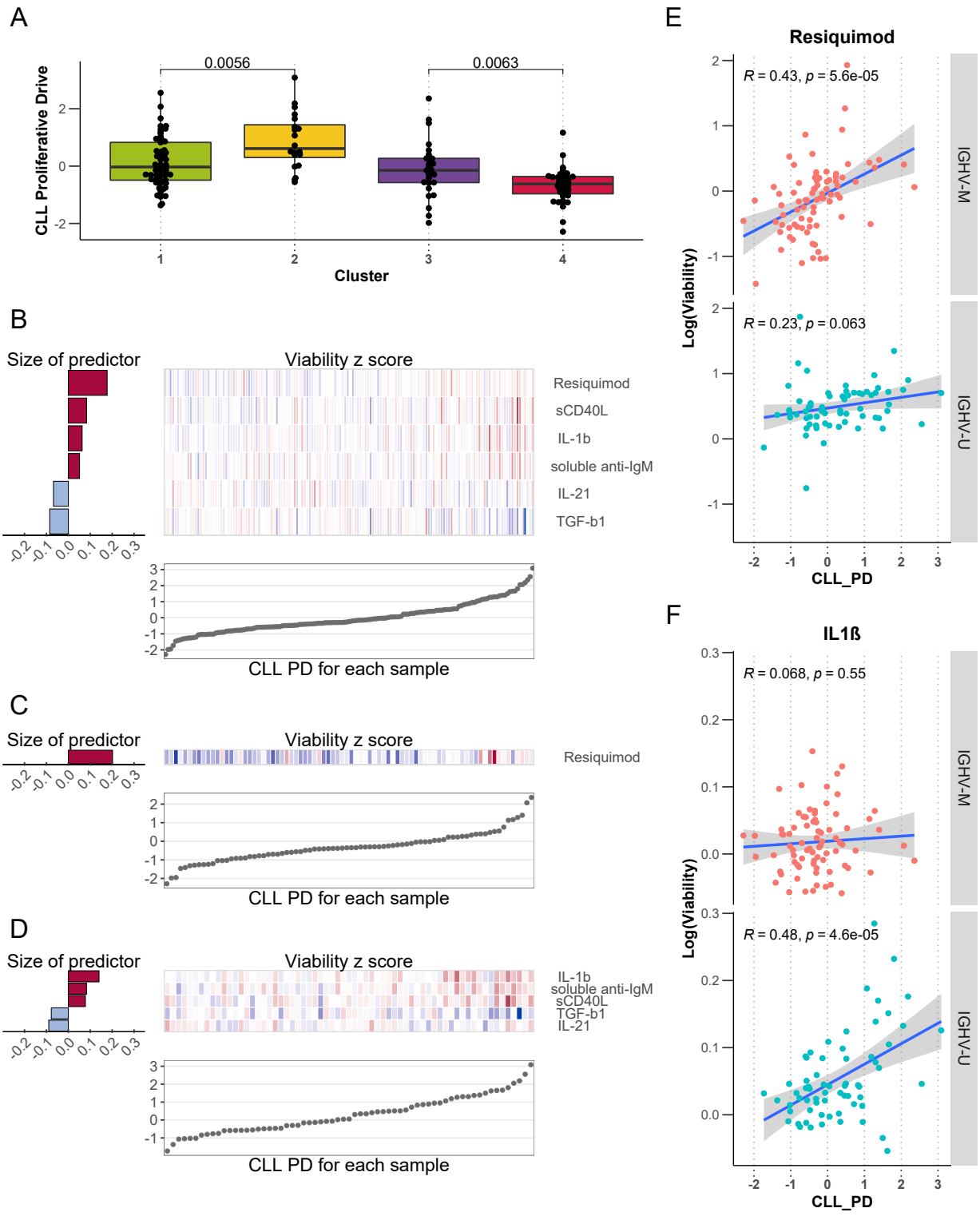

Appendix Figure 6. CLL Proliferative Drive as defined by Lu et al., 2021[5].

Beeswarm Plot of Proliferative drive in the clusters defined by microenvironmental resonse. P-values are shown from student's t-tests. **(A)** Predictor profiles for stimuli response to represent CLL Proliferative Drive

identified through multivariate analysis using Gaussian linear modelling with L1-penalty for all patient samples which were analysed **(B)**, for only IGHV mutated **(C)** and for only IGHV unmutated patient samples **(D)** Within the plots, the bar plots on left indicate size and sign of coefficients assigned to the named predictors. Positive coefficients indicate higher viability after stimulation if the feature is present. Scatter plots indicate log(viability) values, in order of magnitude, for each individual sample. Heatmaps show status for each of the genetic predictors for corresponding sample in scatter plot. Exemplary scatter plots devided by IGHV mutation status shown for Resiquimod **(E)** and IL1ß **(F)**. CLL-PD on x-axis and log normalised viability after microenvironmental stimulation on y-axis. Person correlation coefficients are shown with p-values.

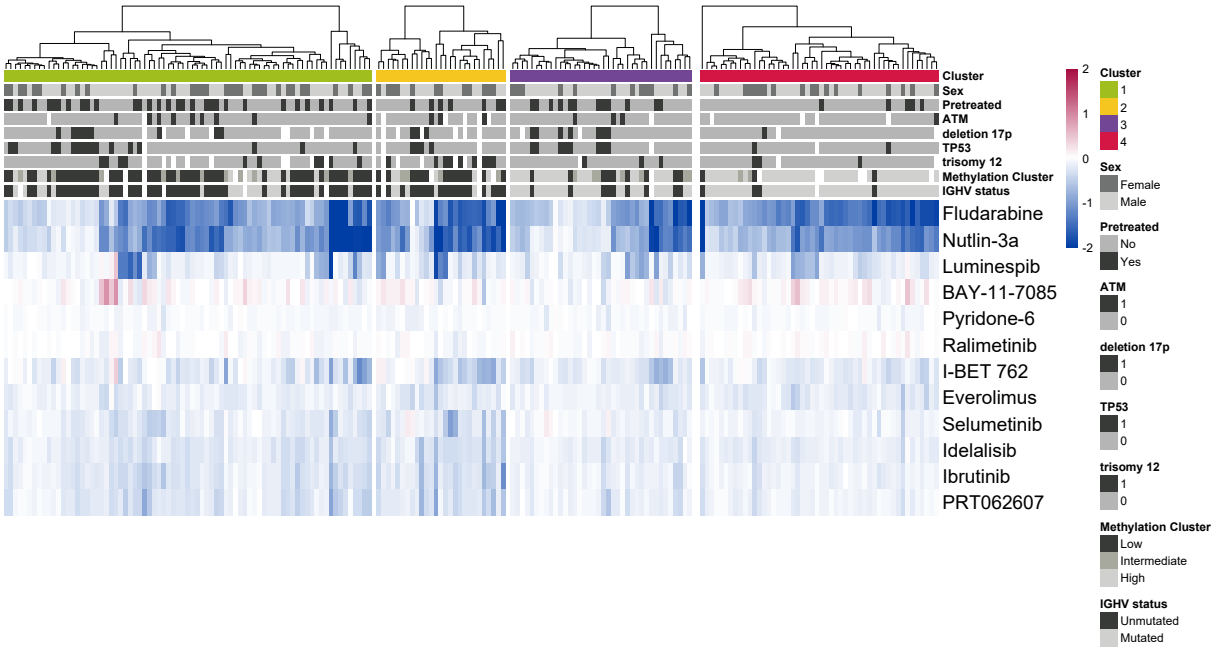

Appendix Figure 7. Drug response between clusters.

Heatmap showing the log normalised viability after drug treatment. Rows represent drug treatments and columns represent primary CLL samples, annotated for their genetic background, sex and pretreatment status above. Red values indicate increased viability upon treatment, blue indicates decreased viability.

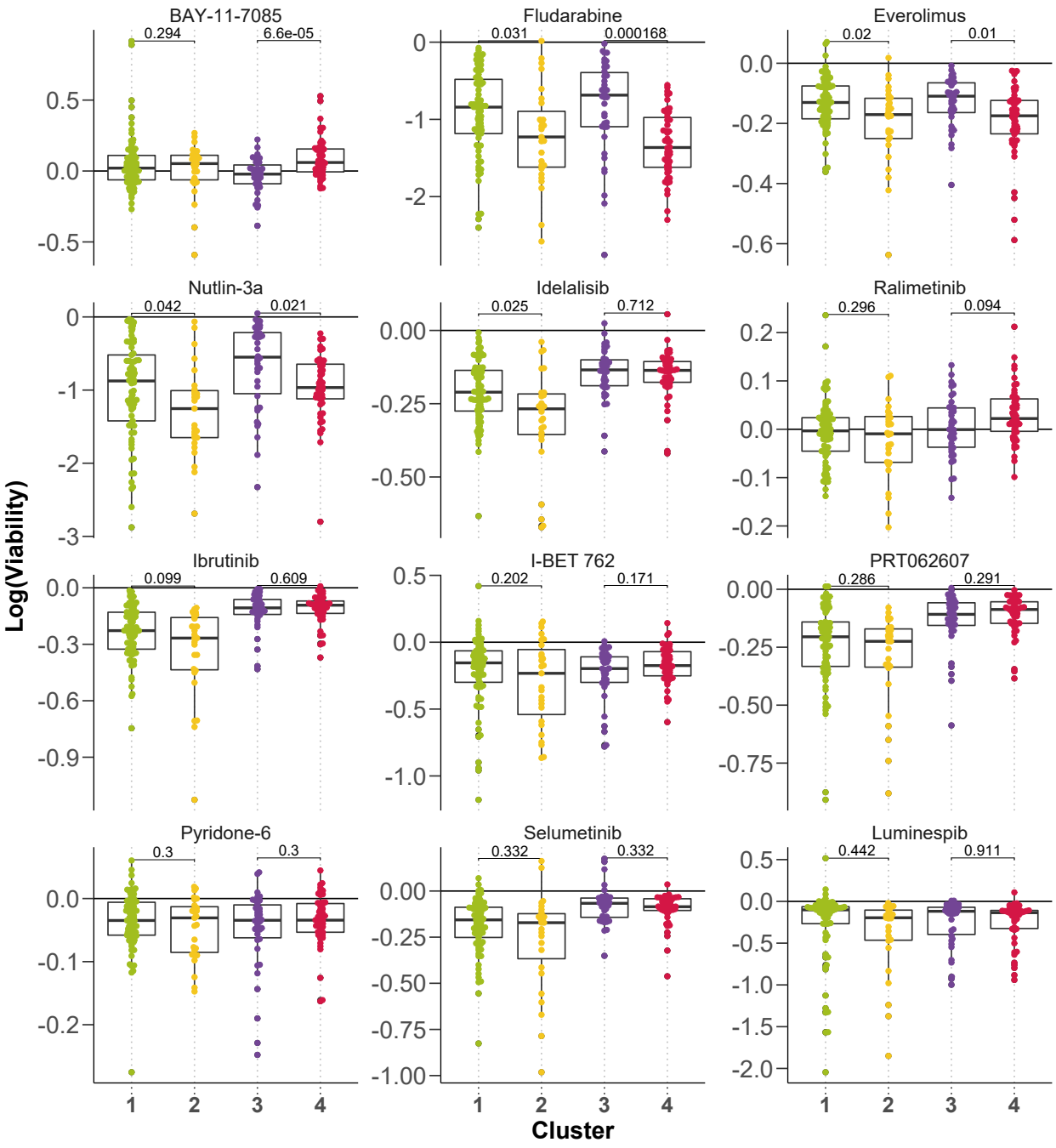

Appendix Figure 8. Drug response by clusters.

Log transformed viabilities after treatment with drugs, faceted by cluster. BH-adjusted p-values from student's t-tests are shown.

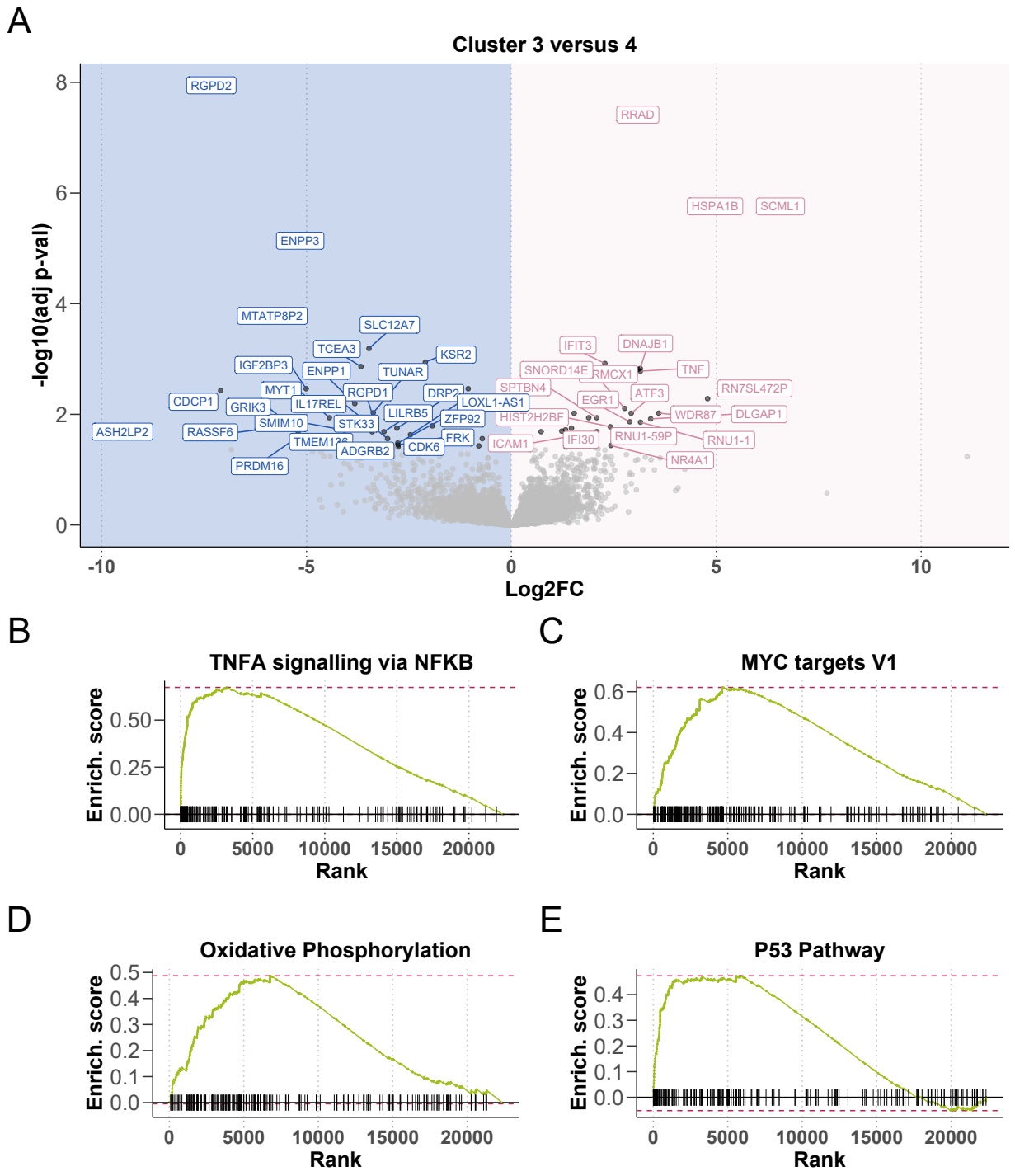

Appendix Figure 9. RNA-Sequencing of matched samples indicates differential gene expression between Cluster 3 and Cluster 4.

Volcano plot of differentially expressed genes between Cluster 3 and Cluster 4 **(A)**. X axis indicates log2 fold change values, calculated using the DESeq2 package, y axis gives corresponding -log10(adjusted p value). P values adjusted using BH method. Genes are labeled where p value < 0.05. Enrichment plots of selected pathways **(B-D)**. Gene set enrichment analysis (GSEA) was performed with the Hallmark gene

sets from the GSEA Molecular Signatures Database. Wald statistic was used to rank the genes. The green curve corresponds to the Enrichment Score curve, which is the running sum of the weighted enrichment score obtained from GSEA software.

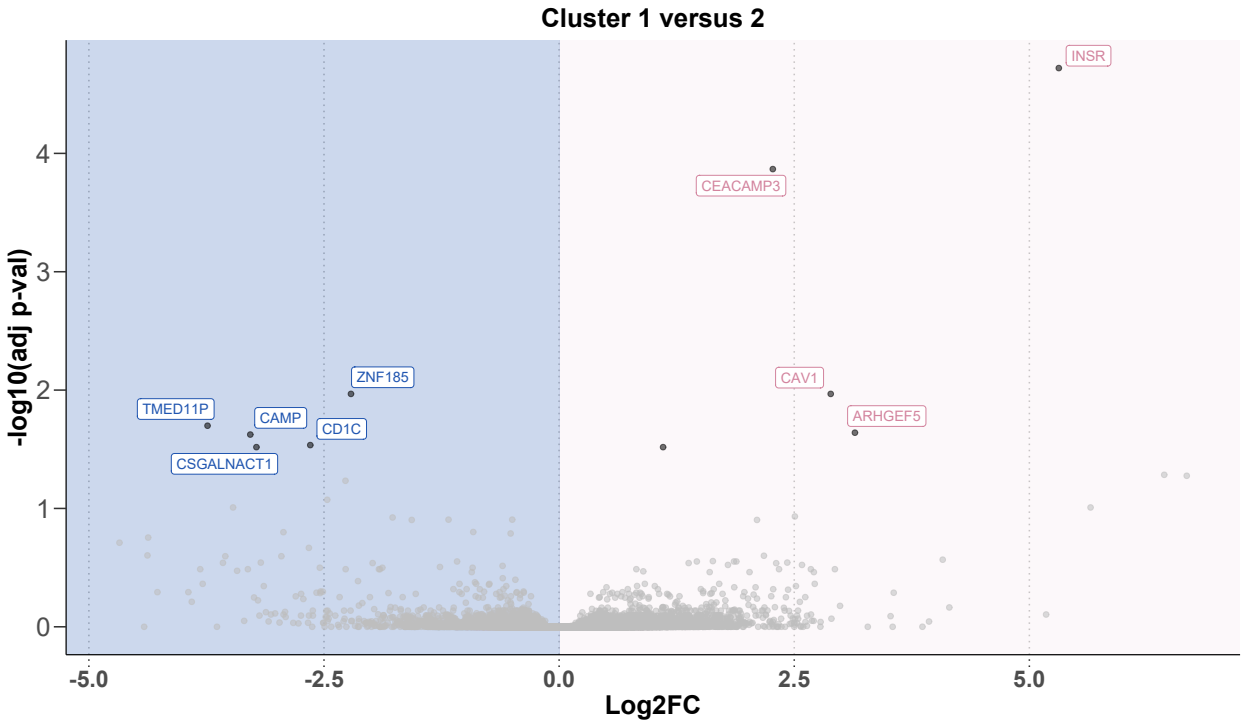

Appendix Figure 10. Comparison of gene expression between Cluster 1 and 2.

Volcano plot of differentially expressed genes between Cluster 1 and Cluster 2. X axis indicates log2 fold change values, calculated using the DESeq package, y axis gives corresponding -log10(adjusted p value). P values adjusted using BH method. Genes are labeled where p value < 0.05.

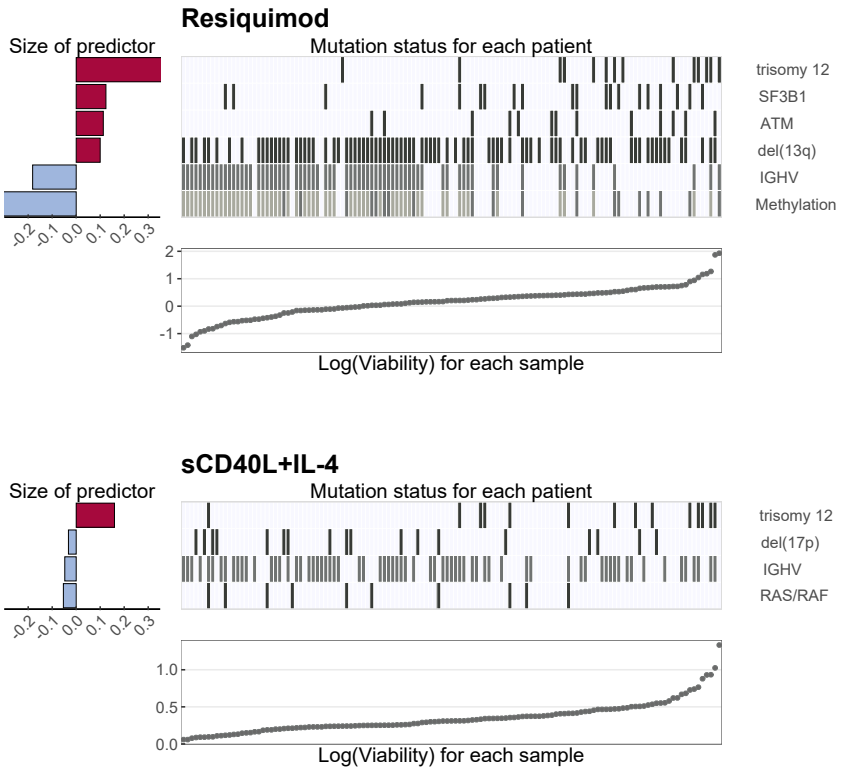

Appendix Figure 11. Predictor profiles to represent gene - stimulus associations.

Stimuli which are not shown in Figure 3B but have predictors >0.02 assigned by multivariate analysis using Gaussian linear modelling with L1-penalty are shown. Within the plots, the bar plots on left indicate size and sign of coefficients assigned to the named predictors. Positive coefficients indicate higher viability after stimulation if the feature is present. Scatter plots indicate log(viability) values, in order of magnitude, for each individual sample. Heatmaps show status for each of the genetic predictors for corresponding sample in scatter plot.

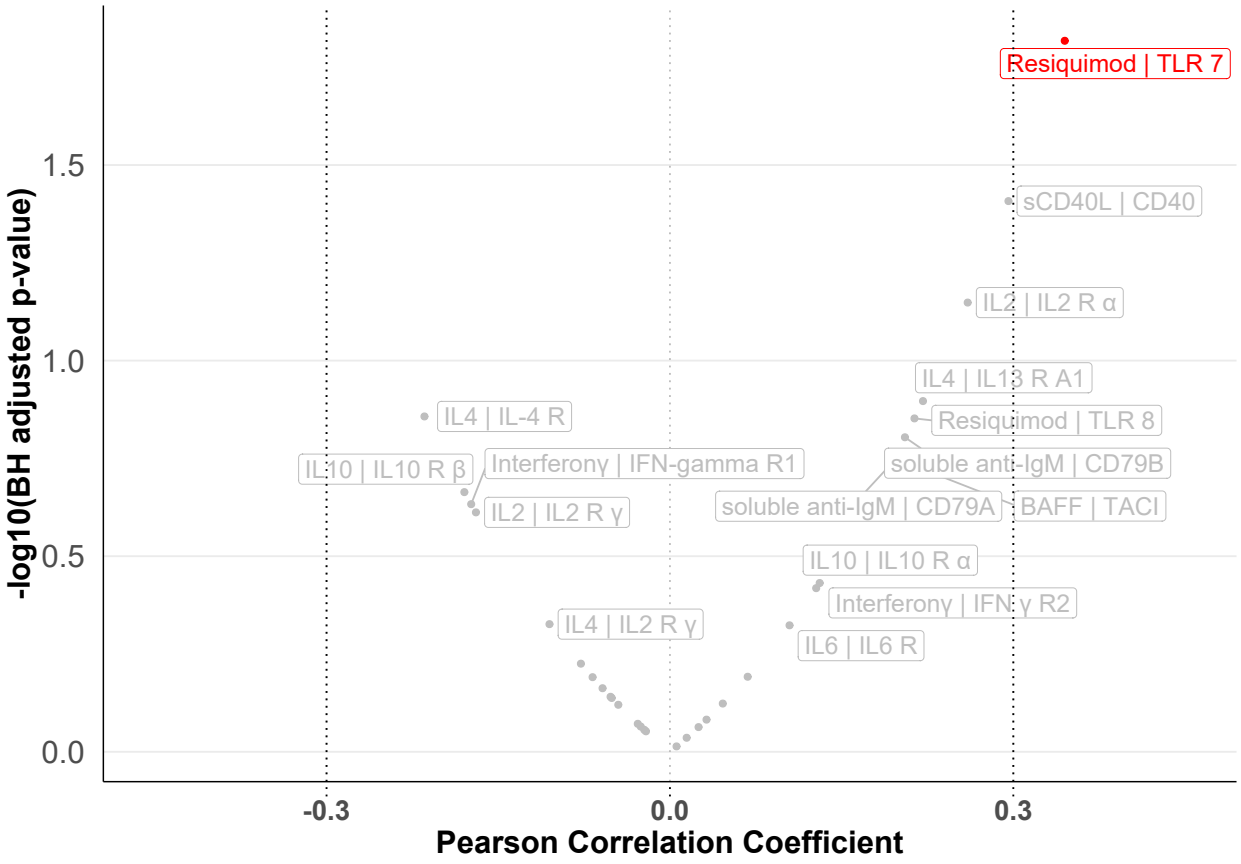

Appendix Figure 12. Correlation of stimuli response and receptor expression.

The effects of the microenvironmental stimuli on viability were largely independent of the expression of the corresponding stimuli receptors. Volcano plot depicts Pearson correlation coefficients against corresponding BH-adjusted p values, for the correlation between control - normalised log viability values with each stimulus and vst RNA counts of corresponding stimuli receptor. RNA counts taken from RNA-Sequencing of untreated matched CLL patient sample. Only viability after treatment with Resiquimod correlated with receptor expression (R>0.3).

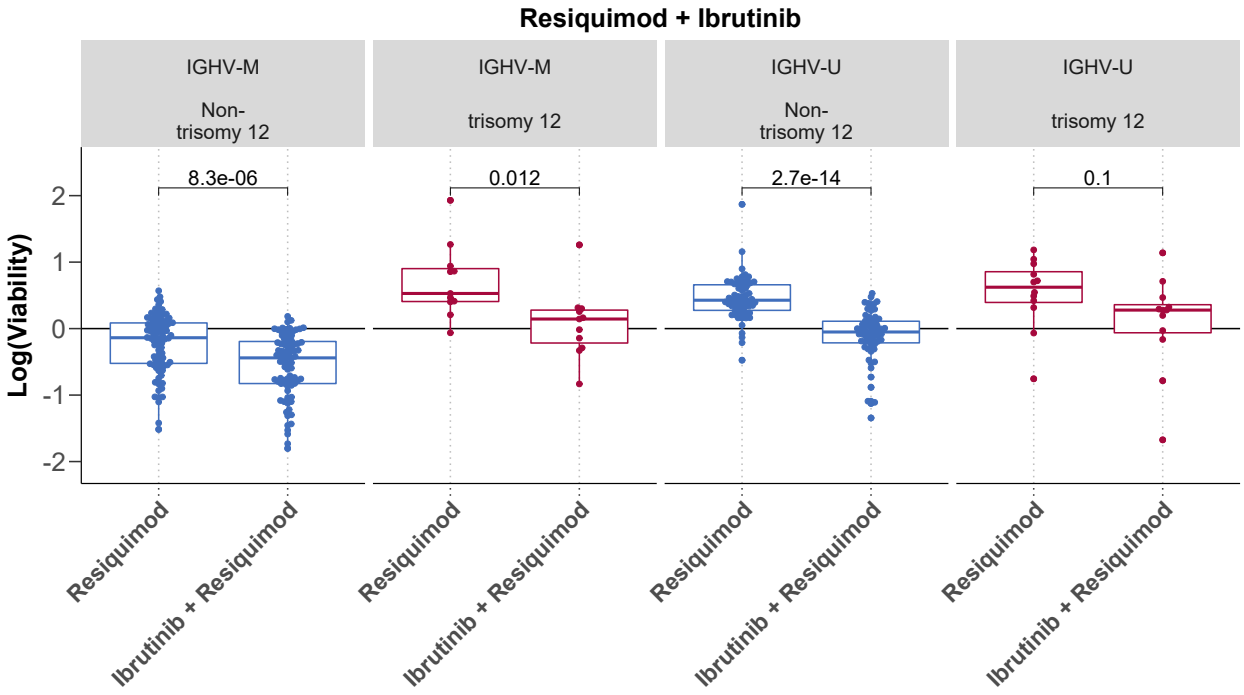

Appendix Figure 13. BCR inhibition by ibrutinib counters the protective effect of TLR stimulation in all genetic subgroups of IGHV and trisomy 12.

Log normalised viability after treatment with Resiquimod with and without ibrutinib. Faceted by IGHV mutation status and trisomy 12.

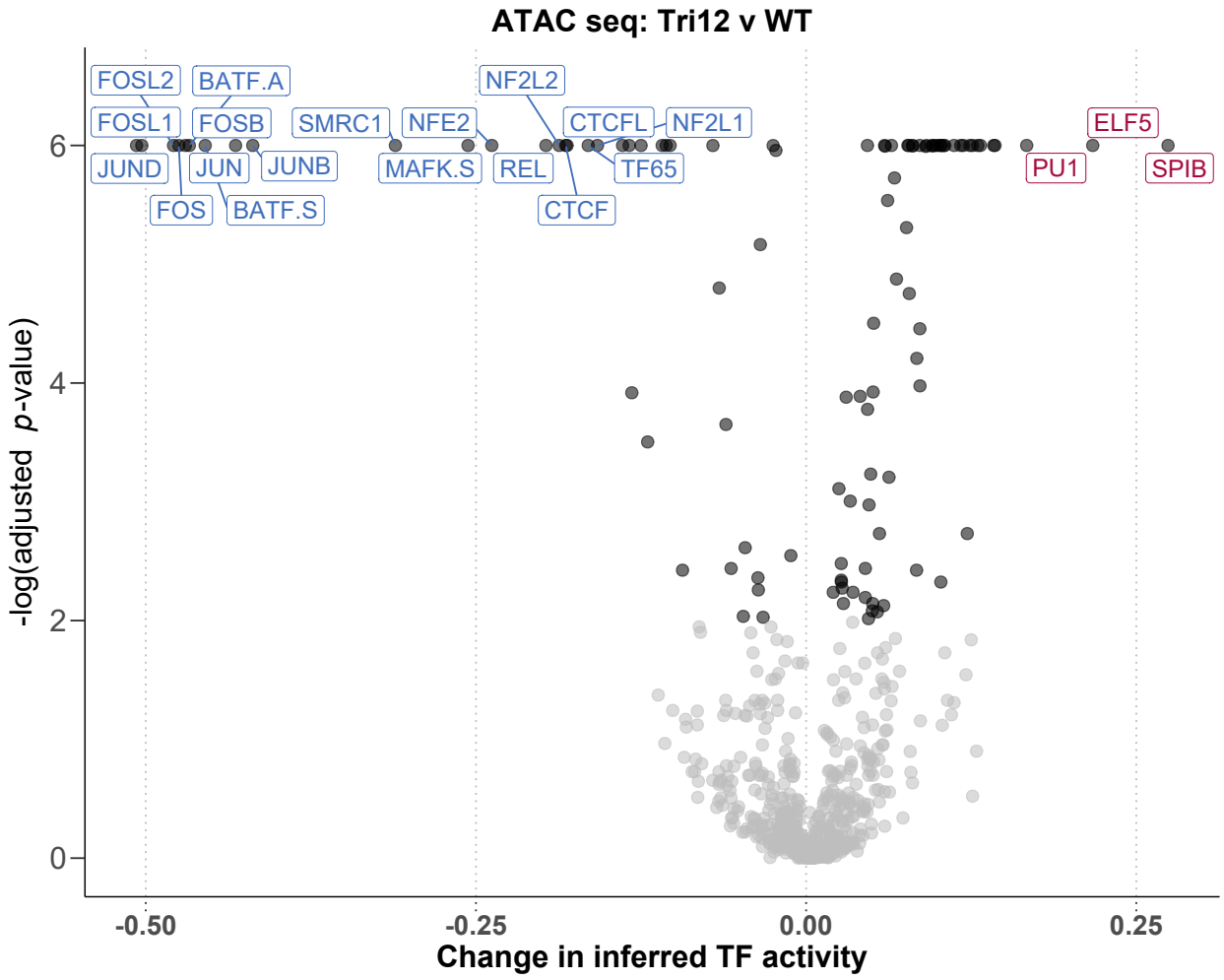

Appendix Figure 14. ATACseq comparing trisomy 12 and non-trisomy 12 CLL samples.

Volcano plot shows change in inferred TF activity (x axis) against adjusted p-values (y axis) for trisomy 12 (n = 2) versus non-trisomy 12 samples (n = 2). Inferred TF activity calculated using the diffTF package, and measured as weighted mean difference. p-values are obtained through diffTF in analytic mode and adjusted by the Benjamini-Hochberg procedure. TFs are labeled where absolute weighted mean difference > 0.15, and adjusted p-value < 0.01.

Appendix Figure 15. ATACseq comparing trisomy 12 and non-trisomy 12 CLL samples.

Volcano plot shows change in inferred TF activity (x axis) against adjusted p-values (y axis) for trisomy 12 (n = 2) versus non-trisomy 12 samples (n = 2). Inferred TF activity calculated using the diffTF package, and measured as weighted mean difference. p-values are obtained through diffTF in analytic mode and adjusted by the Benjamini-Hochberg procedure. TFs are labeled where absolute weighted mean difference > 0.15, and adjusted p-value < 0.01. Data from Beekman et al. 2018.

A

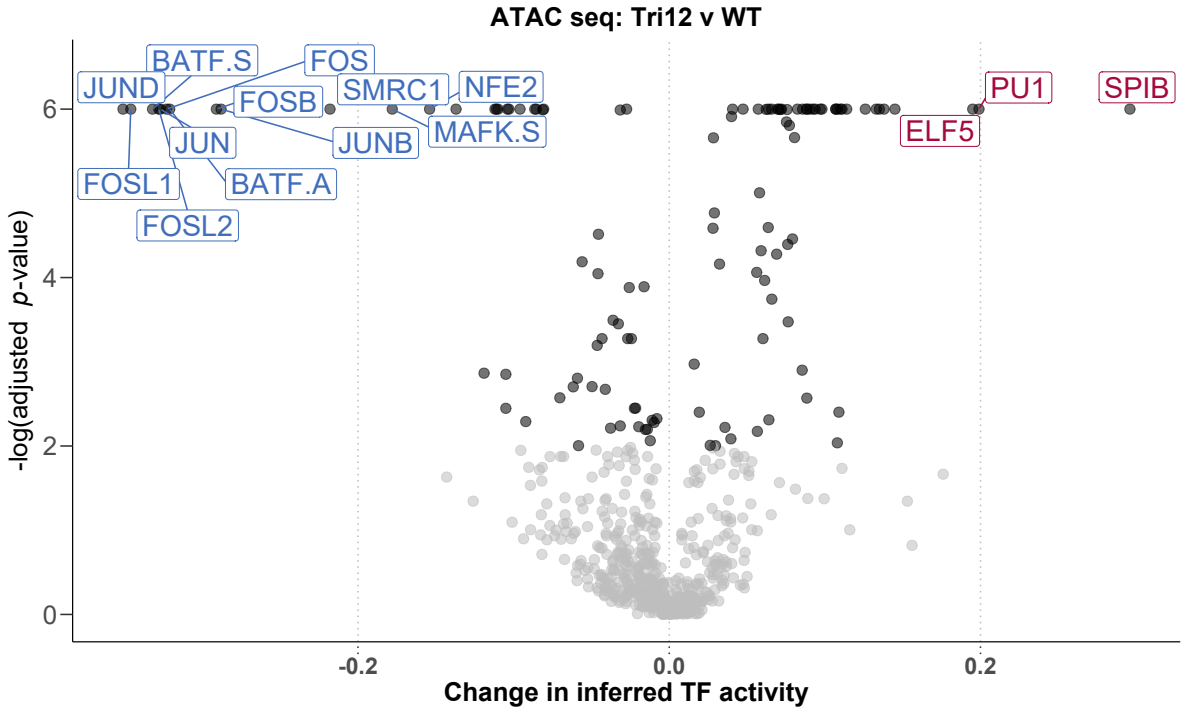
ATAC seq: Tri12 v WT
BATF.S
FOS
JUND
SMRC1
NFE2
FOSB
PU1
SPIB
MAFK.S
ELF5
JUNB
JUN
FOSL1
BATF.A
FOSL2
-log(adjusted p-value)
6
4
2
0
-0.2
0.0
0.2
Change in inferred TF activity

B

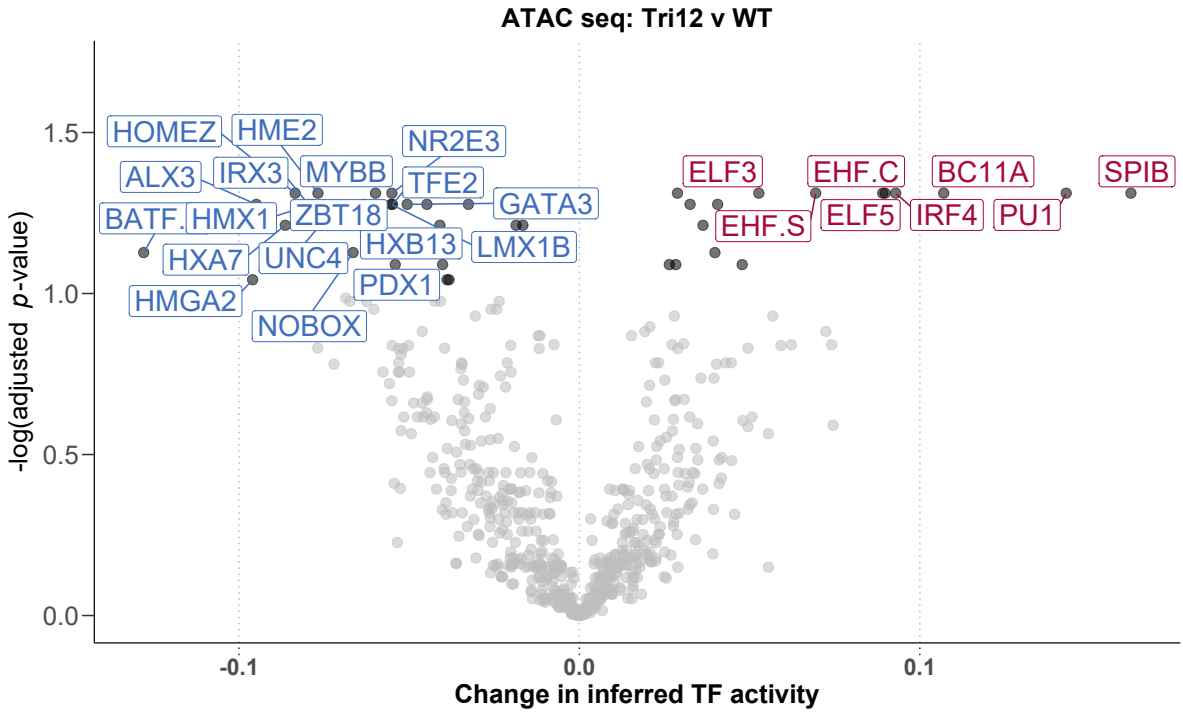
ATAC seq: Tri12 v WT
HOMEZ
HME2
NR2E3
ELF3
EHF.C
BC11A
SPIB
ALX3
IRX3
MYBB
TFE2
GATA3
EHF.S
ELF5
IRF4
PU1
BATF.
HMX1
ZBT18
HXB13
LMX1B
HXA7
UNC4
PDX1
HMGA2
NOBOX
-log(adjusted p-value)
1.5
1.0
0.5
0.0
-0.1
0.0
0.1
Change in inferred TF activity

Appendix Figure 16. ATACseq comparing trisomy 12 and non-trisomy 12 CLL samples, without including TF binding sites on chromosome 12.

Volcano plot shows change in inferred TF activity (x axis) against adjusted p-values (y axis) for trisomy 12 versus non-trisomy 12 samples, for (A) the 2 versus 2 comparison and (B) the 9 versus 42 comparison based on the data from Rendeiro et al. 2016. Inferred TF activity calculated using the diffTF package, and measured as weighted mean difference. p-values are obtained through diffTF in (A) analytic mode and (B) permutation mode, adjusted by the Benjamini-Hochberg procedure. TFs are labelled in (A) where absolute weighted mean difference > 0.15, and adjusted p-value < 0.01 and in (B) where absolute weighted mean difference > 0.05, and adjusted p-value < 0.1.

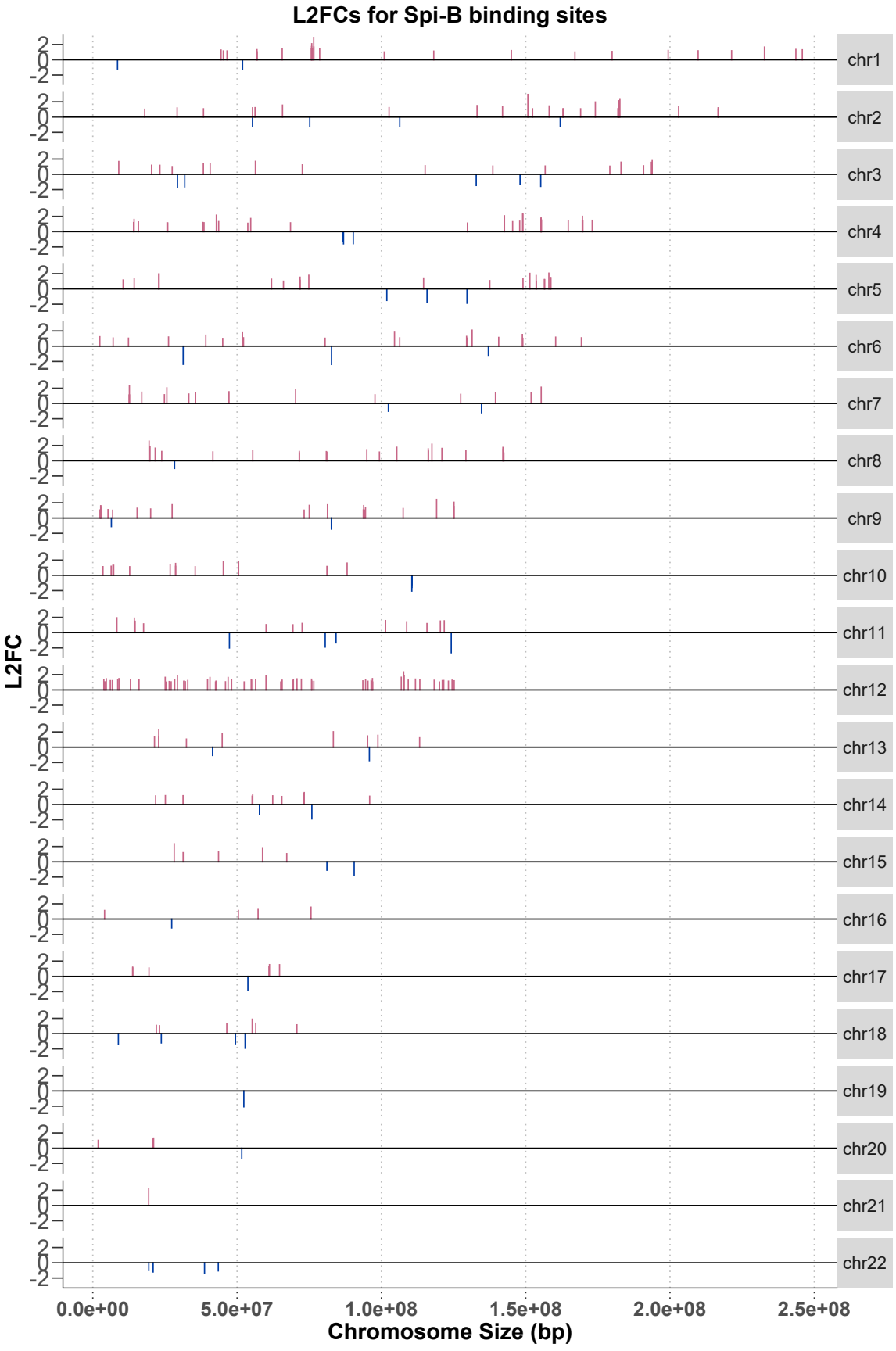
L2FCs for Spi-B binding sites
L2FC
2
0
-2
chr1
chr2
chr3
chr4
chr5
chr6
chr7
chr8
chr9
chr10
chr11
chr12
chr13
chr14
chr15
chr16
chr17
chr18
chr19
chr20
chr21
chr22
0.0e+00
5.0e+07
1.0e+08
1.5e+08
2.0e+08
2.5e+08
Chromosome Size (bp)

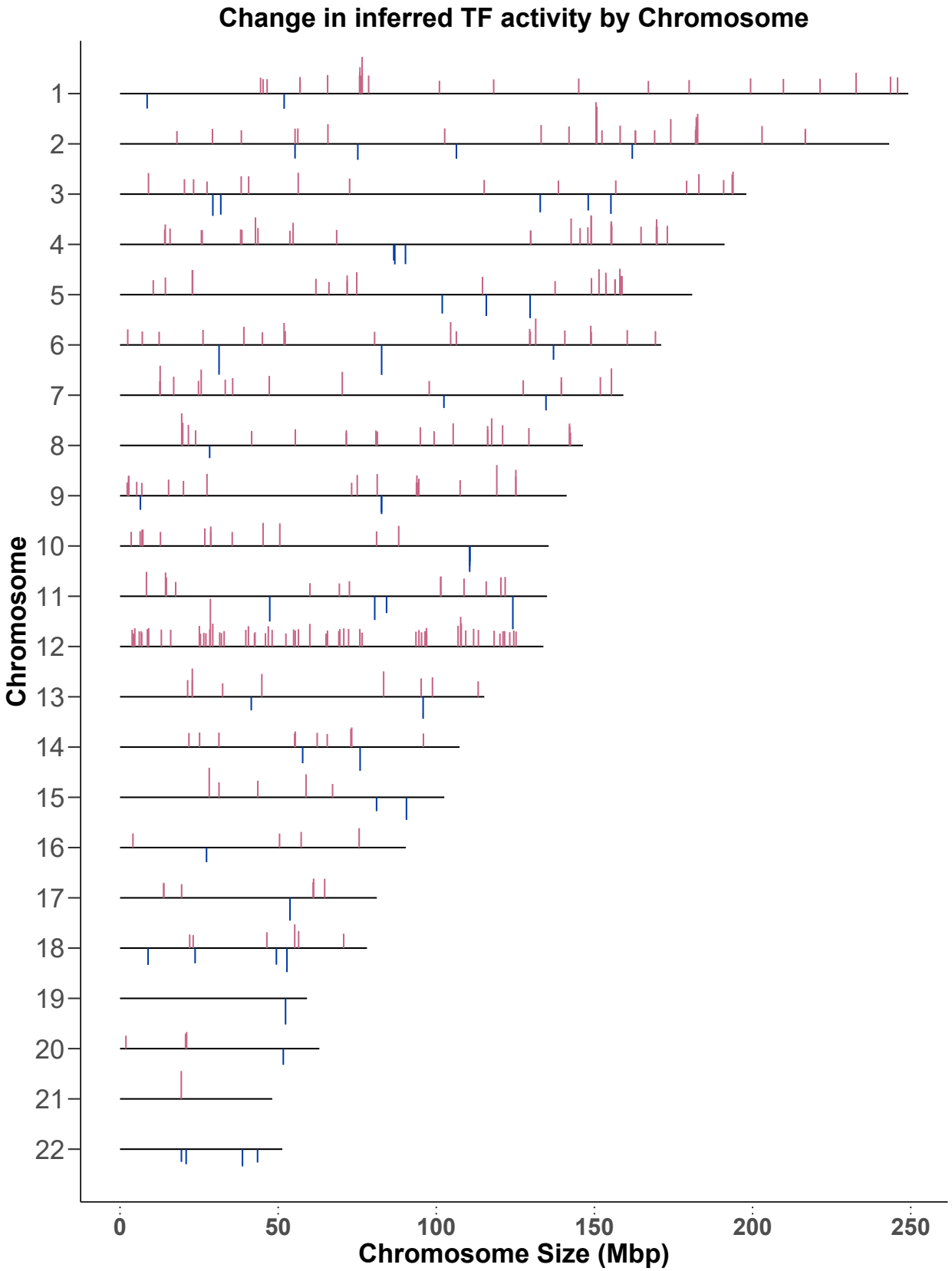
Change in inferred TF activity by Chromosome
Chromosome
1
2
3
4
5
6
7
8
9
10
11
12
13
14
15
16
17
18
19
20
21
22
0
50
100
150
200
250
Chromosome Size (Mbp)

Appendix Figure 17. Chromosomal locations of Spi-B binding sites that show differential accessibility between trisomy 12 and non-trisomy 12 CLL.

Log2 fold changes are plotted (y axis) Spi-B binding sites that show an absolute Log2 fold change > 1 and a p value < 0.1, as calculated using the diffTF package for all Spi-B binding sites defined in the HOCOMOCO database. Data shown is the 9 versus 42 comparison based on the data from Rendeiro et al. 2016.

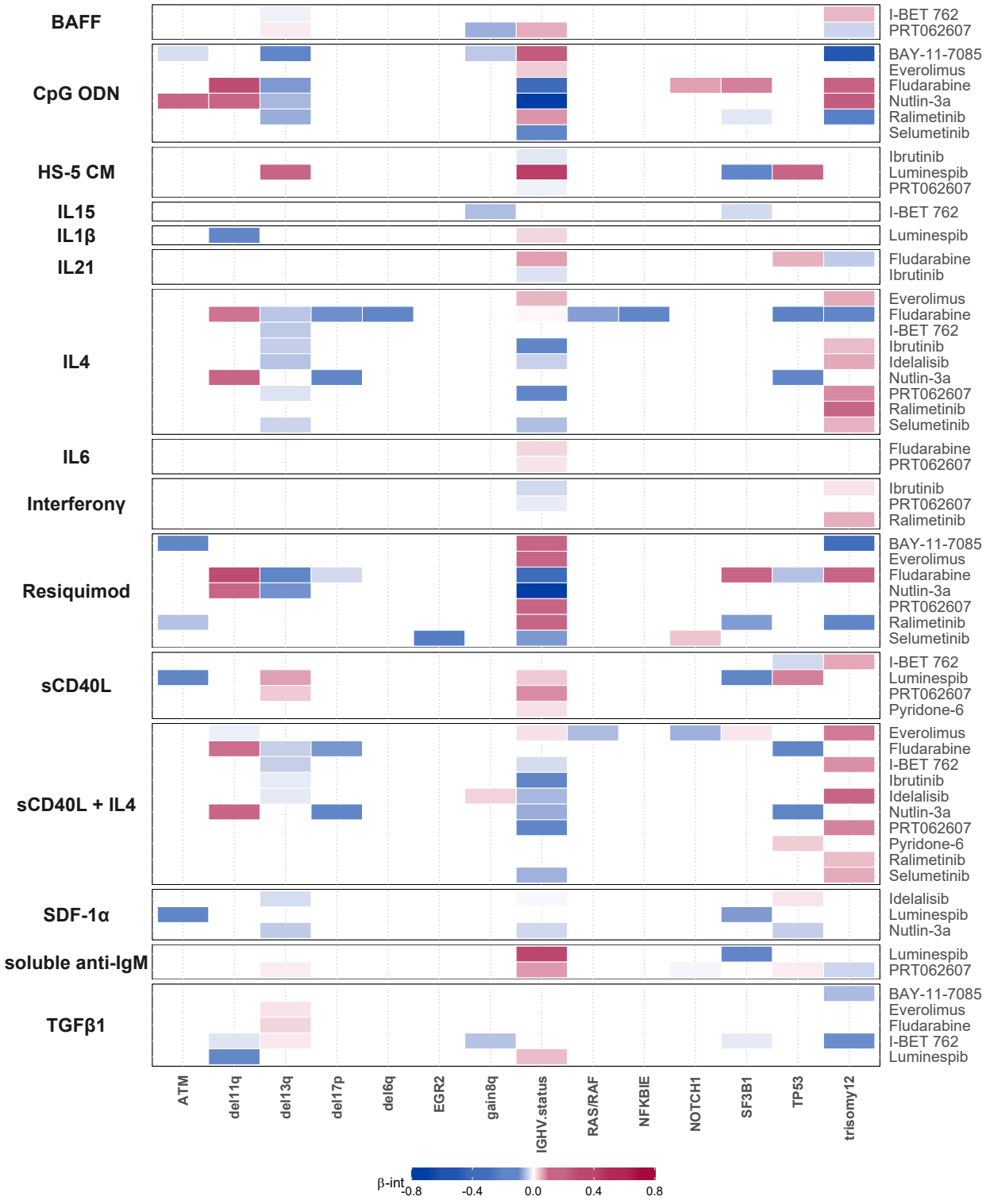

Appendix Figure 18. Genetic predictors of drug - stimulus interactions.

Heatmap depicting overview of genetic predictors of drug - stimulus interactions (each row represents the coefficients from fitting a single multivariate model). Stimuli are shown on left, and corresponding drugs on right. Drugs, stimuli and genetic alterations are alphabetically sorted. Coloured fields indicate that the β_{int}

for given drug and stimulus is modulated by corresponding genetic feature. Positive coefficients are shown in red, indicating β_{int} is more positive for given drug and stimulus combination if the feature is present.

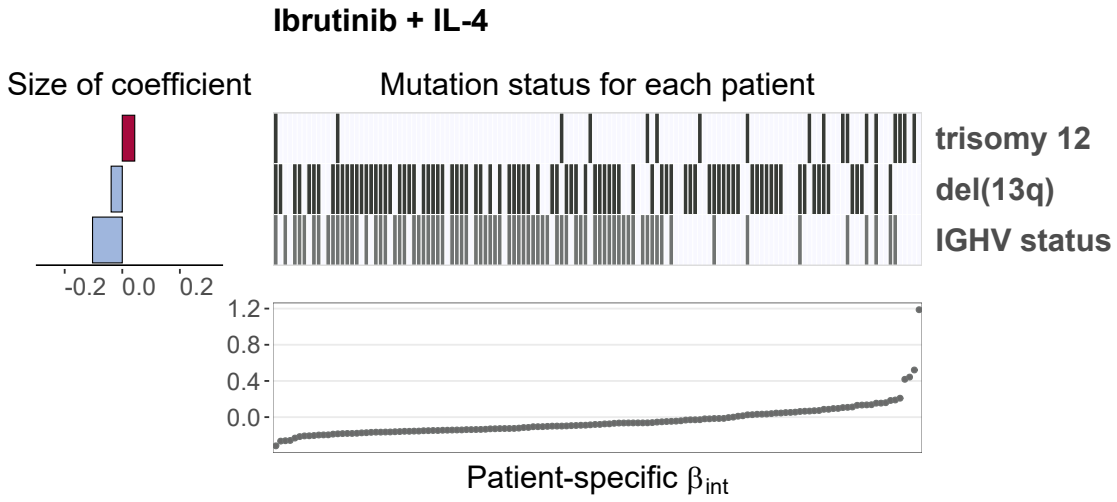

Appendix Figure 19. Genetic predictors of the interaction between ibrutinib and IL4.

Predictor profile depicting genetic features that modulate the size of β_{int} for ibrutinib and IL4. To generate predictor profile, linear model in Eqn. (1) was fitted in a sample - specific manner, to calculate drug-stimulus interaction coefficients (β_{int}) for each patient sample. Ranked patient-specific β_{int} values are shown in lower scatter plot. Associations between the size of β_{int} and genetic features were identified using multivariate regression with L1 (lasso) regularisation, with gene mutations and IGHV status as predictors, and selecting coefficients that were chosen in >90% of bootstrapped model fits. The horizontal bars on left show the size of fitted coefficients assigned to genetic features. Matrix above scatter plot indicates patient mutation status for the selected genetic features. Matrix fields correspond to points in scatter plot (ie patient data is aligned), to indicate how the size of β_{int} varies with selected genetic feature.

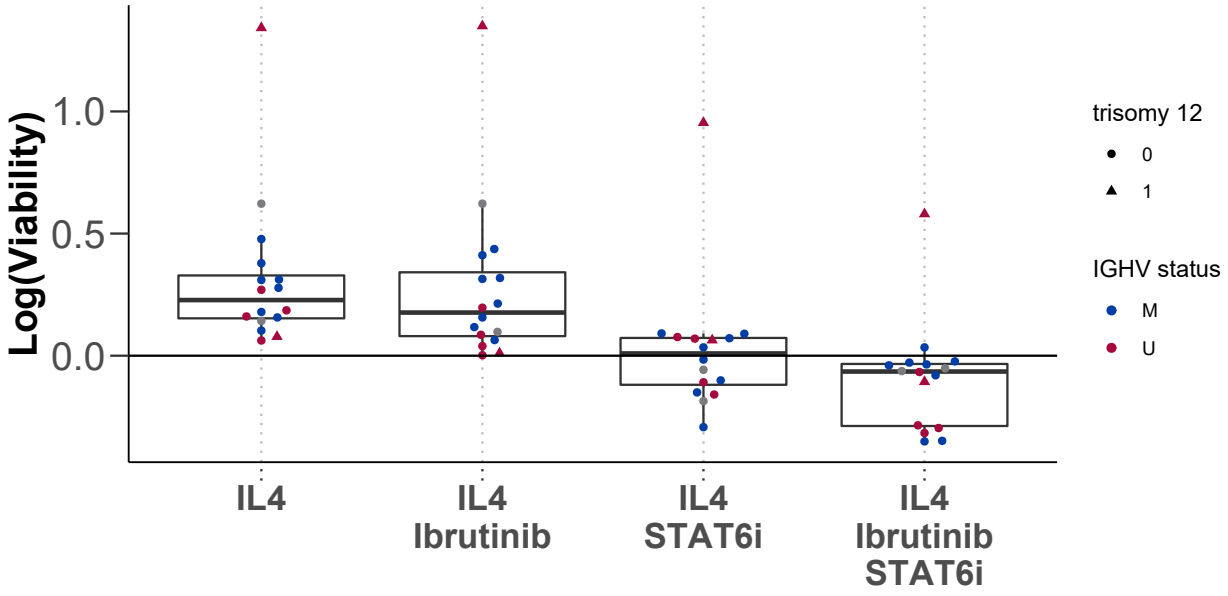

Appendix Figure 20. STAT6 dependency of IL4 signaling.

The effects observed with IL4 stimulation are dependent on STAT6 activation. Addition of the STAT6 inhibitor AS1517499 could revoke the effect on baseline viability as well as drug induced toxicity. Log transformed viability after treatment with IL4 in combination with ibrutinib, the STAT6 inhibitor AS1517499, and both.

References

1. Dietrich S, Oleś M, Lu J, et al. Drug-perturbation-based stratification of blood cancer. J. Clin. Invest. 2018;128(1):427–445.
2. Buenrostro JD, Wu B, Chang HY, Greenleaf WJ. ATAC-seq: A Method for Assaying Chromatin Accessibility Genome-Wide. Curr. Protoc. Mol. Biol. 2015;109:21.29.1–21.29.9.
3. Berest I, Arnold C, Reyes-Palomares A, et al. Quantification of Differential Transcription Factor Activity and Multiomics-Based Classification into Activators and Repressors: diffTF. Cell Rep. 2019;29(10):3147–3159.e12.
4. Kulakovskiy IV, Vorontsov IE, Yevshin IS, et al. HOCOMOCO: expansion and enhancement of the collection of transcription factor binding sites models. Nucleic Acids Res. 2016;44(D1):D116–25.
5. Lu, J., Cannizzaro, E., Meier-Abt, F. et al. Multi-omics reveals clinically relevant proliferative drive associated with mTOR-MYC-OXPHOS activity in chronic lymphocytic leukemia. Nat Cancer 2, 853–864 (2021).